Progressive Retinal Degeneration in Transgenic Mice with Overexpression of Endothelin-1 in Vascular Endothelial Cells

Xue-Song Mi,[1] *Xu Zhang,*[1] *Qian Feng,*[1] *Amy Cheuk Yin Lo,*[3] *Sookja Kim Chung,*[*,1] *and Kwok-Fai So*[*,1,2,4]

Purpose. Endothelin-1 (ET-1), synthesized in vascular endothelial cells, is a potent vasoconstrictor. ET-1–related vascular abnormality has been known to be important in the pathogenesis of glaucoma, especially in normal tension glaucoma. However, the long-term effect of increased vascular ET-1 on the retinal tissue is still unclear.

Methods. The mice with overexpression of ET-1 in vascular endothelial cells (TET-1 mice) were examined with the profile of intraocular pressure (IOP), retinal layer thickness, numbers of retinal ganglion cells (RGCs), and axonal changes associated with blood vessel changes.

Results. The TET-1 mice exhibited a significant progressive loss of RGCs and decrease of retinal thickness in the inner nuclear layer (INL) and outer nuclear layer (ONL) as early as around 10–12 months. At 24 months, the retinal degeneration became more severe, with around 30% RGC loss associated with thinning of the retinal nerve fiber layer and there was an increase in neuronal loss and thinning of the INL and ONL. In the 24-month-old TET-1 mice, IgG leakage in the blood vessels and decrease in the occludin protein were observed. There was increased glial fibrillary acidic protein expression in the Müller cells. In addition, the astrocytic end-feet on blood vessels were enlarged. The IOP level was normal in all ages (1–24 months) of TET-1 mice.

Conclusions. These data suggested that TET-1 mice may be a useful model to address endothelial ET-1–related mechanisms in vascular-associated retinal degenerative diseases. (*Invest Ophthalmol Vis Sci.* 2012;53:4842–4851) DOI:10.1167/iovs.12-9999

From the [1]Department of Anatomy and the State Key Laboratory of Brain and Cognitive Science, Hong Kong, China; the [2]Research Centre of Heart, Brain, Hormone and Healthy Aging, Hong Kong, China; the [3]Eye Institute, Li Ka Shing Faculty of Medicine, The University of Hong Kong, Pokfulam, Hong Kong, China and [4]The Joint Laboratory for Brain Function and Health, Jinan University and The University of Hong Kong, Guangzhou, China.

Supported in part by a General Research Fund grant from Hong Kong Research Grant Council, National Basic Research Program of China Grant 2011CB707501, and the Fundamental Research Funds for The Central Universities Grant 21609101.

Submitted for publication April 10, 2012; revised May 28, 2012; accepted June 15, 2012.

Disclosure: **X.-S. Mi**, None; **X. Zhang**, None; **Q. Feng**, None; **A.C.Y. Lo**, None; **S.K. Chung**, None; **K.-F. So**, None

*Each of the following is a corresponding author: Kwok-Fai So, Department of Anatomy, Li Ka Shing Faculty of Medicine, The University of Hong Kong, Pokfulam, Hong Kong, China; hrmaskf@hkucc.hku.hk.

Sookja Kim Chung, Department of Anatomy, Li Ka Sing Faculty of Medicine, The University of Hong Kong, Pokfulam, Hong Kong, China; skchung@hkucc.hku.hk.

Glaucoma, an irreversible blindness-inducing disease affecting individuals worldwide, is a neurodegenerative disease of the eye.[1] Normal-tension glaucoma (NTG), a subtype of primary open-angle glaucoma (POAG), shares similar features of neurodegeneration with POAG, although without the elevation of IOP. Epidemiologic studies showed that NTG could contribute to a large portion of all POAG in some races,[2,3] suggesting that IOP-independent factors may play key roles in the progressive neurodegeneration of NTG. Clinically, vasospastic disorders, such as migraine headache, Raynaud phenomenon, and ischemic vascular diseases, were shown a higher prevalence among patients with NTG.[4] Together, among these non-IOP–related mechanisms, vascular abnormality may play an important role in the pathogenesis of NTG.

Endothelin-1 (ET-1), a potent vasoconstrictor, has been suggested to be a contributor to the pathophysiology of glaucoma.[5] Clinically, an increased level of ET-1 has been found in circulating plasma of patients with NTG in many studies.[6–8] Moreover, ET-1 was thought to be a link between vascular dysfunctional symptom and patients with NTG.[9,10] In animal models, administration of ET-1 to the eye produced chronic optic nerve ischemia.[11–13] Further comparison of these findings indicated that different delivery methods induced different effects on the retinal neurons; for example, retrobulbar delivery of ET-1 could kill only the retinal ganglion cells (RGCs),[13,14] whereas intravitreal injection of ET-1 not only induces the selective loss of RGCs[15] but also damages the neurons in the inner nuclear layer (INL).[12,16] These phenomena may be attributed to the local effects of ET-1. However, there is no proper animal model yet to mimic the clinical conditions of the long-term effects of increased vascular ET-1 in circulation in some population of patients with NTG.

In this study, we used a transgenic mice line (TET-1) with overexpression of ET-1 in the vascular endothelial cells using the tyrosine kinase receptor specific for endothelial cells (the Tie-1 promoter),[17] to examine the long-term effect of endothelial ET-1 on the morphologic changes in the retina and optic nerve. We further tested the hypothesis that the overexpression of endothelial–ET-1 may be a cause or a contributor in the development of neurodegeneration in the retina.

Methods

Mice

The generation of TET-1 mice was reported previously[17,18] by microinjection of the ET-1 construct, which contains ET-1 cDNA with SV40 polyA driven by the Tie-1 promoter. TET-1 mice, maintained in the F1 hybrid background (C57BL/6J × CBA), and their non-transgenic littermate control (Non-tg) mice were used in this study. The animals were maintained on a 12-hour light/dark cycle and received food and water without restriction. All animal experimental design and

Investigative Ophthalmology & Visual Science, July 2012, Vol. 53, No. 8

Table. Reagent Utilization

Antibody	Dilution	Host	Company	Catalog Number
ET-1	1:1600	Rabbit	Peninsula	T-4050
GS	1:600	Mouse	Millipore	MAB302
GFAP	1:400	Mouse	Sigma	G3893
GFAP	1:1000	Rabbit	Dako	Z0334
β-Tubulin III	1:500	Mouse	Covance	MMS-435P
Alexa Fluor 568 (Goat anti-rabbit)	1:200		Molecular Probes	A11036
Alexa Fluor 488 (Goat anti-mouse)	1:200		Molecular Probes	A11029
Alexa Fluor 350 (Goat anti-rabbit)	1:200		Molecular Probes	A21068
Isolectin B4	1:100		Invitrogen	I21412
MOM kit			Vector Labs	FMK-2201
DAB kit			Invitrogen	002114

protocols were in accordance with the ARVO statement for the Use of Animals in Ophthalmic and Vision Research, and were approved by the Committee for the Use of Live Animals in Teaching and Research (CULATR #1664-08) at The University of Hong Kong.

Retinal Sample Preparation

Animals were euthanized by pentobarbital overdose. The eyeballs were removed immediately, fixed in 4% paraformaldehyde (PFA) overnight at 4°C, dehydrated with a graded series of ethanol and xylene, and subsequently embedded in paraffin wax. With clear orientation of each eyeball, 7-μm-thick cross-sections were cut with a serial code on each slide to ensure that a similar area was used for the morphologic comparison. The optic nerves were collected by cutting at 1.5 mm from the back of the eyeball. The samples were fixed in a mixture of 2% glutaraldehyde and 2% PFA in 0.1 M phosphate buffer (PB) at 4°C overnight. The tissues were then embedded in 2% agar with clear orientation and post-fixed in 1% osmium tetraoxide in 0.1 M PB for 2 hours at 4°C. After dehydration with graded ethanol, the tissues were embedded in a commercial resin (Epon 812 resin; Nisshin EM, Tokyo, Japan). Flat-mounted retinas were prepared by fixing the eyeballs in 4% PFA at 4°C for 1 hour before the retina was isolated.

Histologic Analysis on H&E-Stained Retinal Sections

Based on previous methods,[19,20] to standardize the retinal section for examination, retinal sections with the optic nerve stump were used for hematoxylin and eosin (H&E) staining. At least three discontinuous sections with optic nerve stump were chosen. Four images under ×400 amplification were taken from a retinal section at the central retina (200 μm from the optic nerve head) and peripheral retina (200 μm from the peripheral edge) using a bright-field microscope (Axiophot 2; Carl Zeiss Microscopy GmbH, Jena, Germany). Then the number of neurons was counted to estimate the density of neurons in the ganglion cell layer (GCL) (per mm). The retinal layer thickness, including the nerve fiber layer (NFL), inner nuclear layer (INL), and outer nuclear layer (ONL), was measured using commercial software (Stereo Investigator; MBF Bioscience [MicroBrightField, Inc.], Williston, VT). Briefly, at least four measurements were taken randomly in a microscopic field, and then an average was calculated to yield the thickness of the corresponding layer.

Morphologic Examination of the Optic Nerve Head

The H&E-stained retinal sections with optic nerve stump were used to examine the morphology of optic nerve head. For the resin-embedded (Epon 812) optic nerves, transverse semithin sections (0.5 μm) were stained with 1% toluidine blue in 1.0% sodium borate and then observed under ×1000 amplification (Axiophot 2; Carl Zeiss Microscopy).

Immunocytochemistry (ICC)

ICC staining was performed using the following procedure. Samples were rinsed with PBS and blocked in PBS with 0.3% Triton X-100 and 10% goat serum for 1 hour. Then, they were incubated with primary antibodies at 4°C overnight followed by second antibodies conjugated with different fluorophores (the Table). Retinal cross-sections were incubated with secondary antibody for 2 hours at room temperature. For flat-mounted retinas, secondary antibodies were incubated at 4°C overnight. Retinal wholemounts were then mounted on slides and visualized using a fluorescent microscope (Axiophot 2; Carl Zeiss Microscopy) or confocal laser scanning microscope (LSM 510 Meta; Carl Zeiss Microscopy).

RGC Counting on Flat-Mounted Retinas

The number of β-tubulin III–stained RGCs[21,22] was counted. The counting method has been described previously.[23] Briefly, under a grid of 200 × 200 μm^2 in the eyepiece along the median line of each quadrant, the number of β-tubulin immunopositive cells in six microscopic fields in each quadrant was counted, starting from the optic disc to the border at 400-μm intervals. A total of 24 fields per retina was counted corresponding to approximately 3% of each retina. The data were shown as percentage loss of RGCs by comparing the density between the TET-1 and Non-tg retina.

IgG Extravasations

Retinal sections were prepared as described earlier and blocked with 10% normal goat serum for 1 hour, after which they were incubated with an immunodetection kit (Biotinylated Mouse on Mouse Anti-mouse Kit; Vector Laboratories, Inc., Burlingame, CA) IgG secondary antibody and avidin-biotin-peroxidase complex. The positive immunoreactivity of IgG was detected with diaminobenzidine tetrahydrochloride (DAB).[24]

Analysis of Capillary Network and Arteriole Branch Points on Flat-Mounted Retinas

Using Isolectin B4 staining, the retinal capillary network was assessed, then the densities of the capillary network and the branch points were analyzed as previously reported.[25,26] The superficial retinal vasculature was acquired under a confocal laser scanning microscope (LSM 510 Meta; Carl Zeiss Microscopy). To quantify the density of the capillary network, three ×20 images from the central, midperipheral, and peripheral retina in each quadrant were acquired sequentially. Each field of view (FOV, 200 × 200 μm^2) contented the capillary networks located between one pair of radially oriented arteriole and venule. A total of 12 representative FOVs were taken from four quadrants in each retina for analysis using ImageJ software (developed by Wayne Rasband, National Institutes of Health, Bethesda, MD; available at http://rsbweb.nih.gov/ij/) based on fluorescence intensities ranging

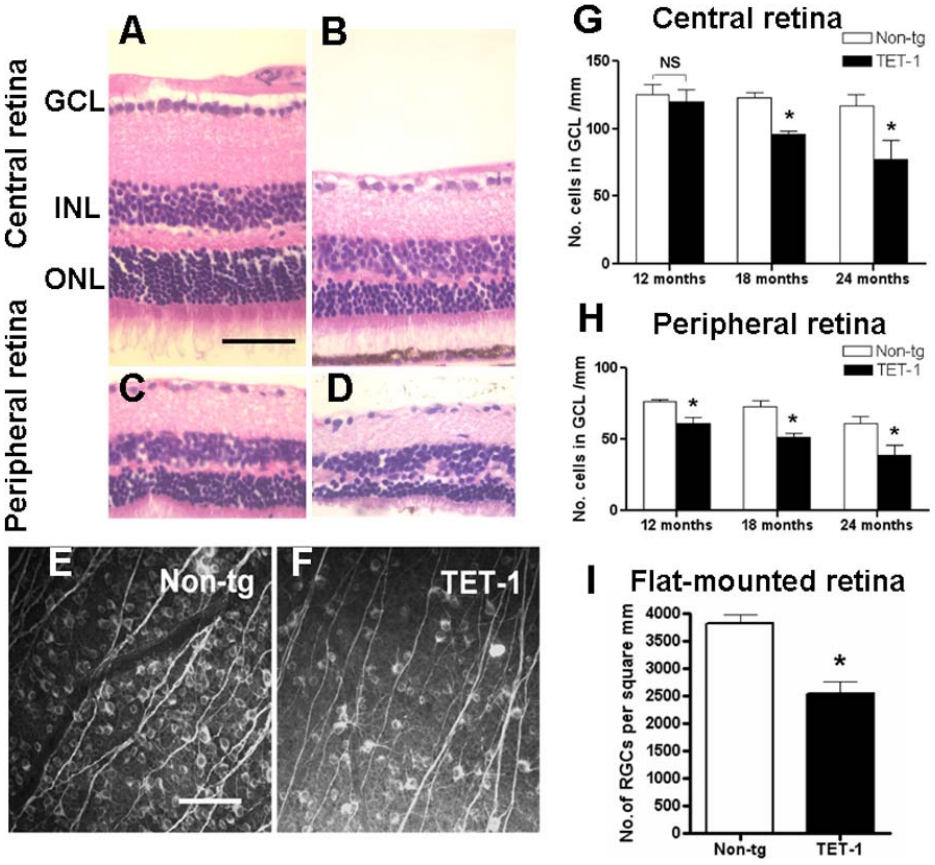

Figure 1. Loss of RGCs in TET-1 mice. (**A**–**D**) Hematoxylin–eosin-stained retinal sections of 24-month Non-tg and TET-1 mice. (**A**) The central retina of Non-tg mice. (**B**) The central retina of TET-1 mice. (**C**) The peripheral retina of Non-tg mice. (**D**) The peripheral retina of TET-1 mice. (**E**, **F**) β-Tubulin III–labeled RGC staining on retinal flat-mounts. (**G**) The analysis of neuronal loss in the central area of GCL ($n = 7$, $^*P < 0.001$). (**H**) The analysis of neuronal loss in the peripheral area of GCL ($n = 7$, $^*P < 0.001$). (**I**) The analysis of β-tubulin III–labeled RGCs on retinal flat-mounts of 24-month Non-tg and TET-1 mice ($n = 7$, $^*P < 0.001$). All scale bars: 50 μm.

from 0 to 255, then the mean optical density was calculated to represent the average capillary density of each retina. For the quantification of vascular branch points, ×10 images were used. In each retinal quadrant, the counting was performed from only one side of branches in the main retinal artery within a single pair of main arteriole and main venule. The number of points in four quadrants of each retina was summed and then divided by the total number of primary branches counted in retinal arterioles and the value obtained was the branch point density of the retina.

Semiquantification of GFAP Staining on Retinal Cross-Sections

The method to collect retinal sections was as described earlier. Three slides (including at least 12 sections) with the same code number and not adjacent to each other were used to ensure the comparison in similar retinal areas among different groups. For image analysis, at least five photographs per section at ×400 amplification were taken randomly under the same fluorescence exposure setting. ImageJ software (http://rsbweb.nih.gov/ij/) was used to obtain the fluorescence intensities and the average value was used to represent the labeling intensity of each retina. This method was based on the criteria published previously.[27]

Western Blotting

The level of occludin in the retina was measured using Western blotting. The retinas (24-month-old of TET-1 and Non-tg mice) were homogenized in lysis buffer (10 mM Tris pH 7.4, 150 mM NaCl, 1 mM EDTA, 1 mM EGTA, 10% protease inhibitor cocktail, and 1% phosphatase inhibitor cocktails) and centrifuged (2000*g*, 5 minutes, 4°C). The supernatant was measured by protein assay kit (Bio-Rad Laboratories, Hercules, CA). A 40 μg aliquot of proteins from each individual animal was subjected to 12.5% SDS–polyacrylamide gel electrophoresis and transferred into a polyvinylidene difluoride membrane. The blot was incubated with antibody against occludin (1:1000; Invitrogen, Carlsbad, CA) and β-actin (1:10,000; Santa Cruz Biotechnology, Santa Cruz, CA). The secondary antibody was horseradish peroxidase–conjugated secondary antibody (Dako Japan Co. Ltd., Kyoto, Japan). Signals were visualized by emitter-coupled logic (ECL; Amersham, Buckinghamshire, UK) and quantitated using ImageJ software. The ratio of occludin expression for TET-1 retina over Non-tg counterparts was determined after normalizing the individual β-actin levels.

Intraocular Pressure (IOP) Monitoring

IOP was measured using a noninvasive rebound tonometer (TONO-LAB; Colonial Medical Supply, Franconia, NH). TET-1 mice and their littermates were grouped by their ages as young (1–2 months), adult (10–12 months), and aged (21–24 months). Both male and female animals were used. Animals were anesthetized with a mixture of ketamine (80 mg/kg) and xylazine (8 mg/kg). Proparacaine hydrochloride 0.5% (Alcaine; Alcon, Ltd., Fort Worth, TX) was also applied to desensitize the cornea. All IOP measurements were taken consistently at approximately 8 to 10 PM to avoid diurnal variations[28] and 10 readings were averaged for each measurement of both right and left eyes. The animals were returned to their cages after the measurements and kept warm for recovery.

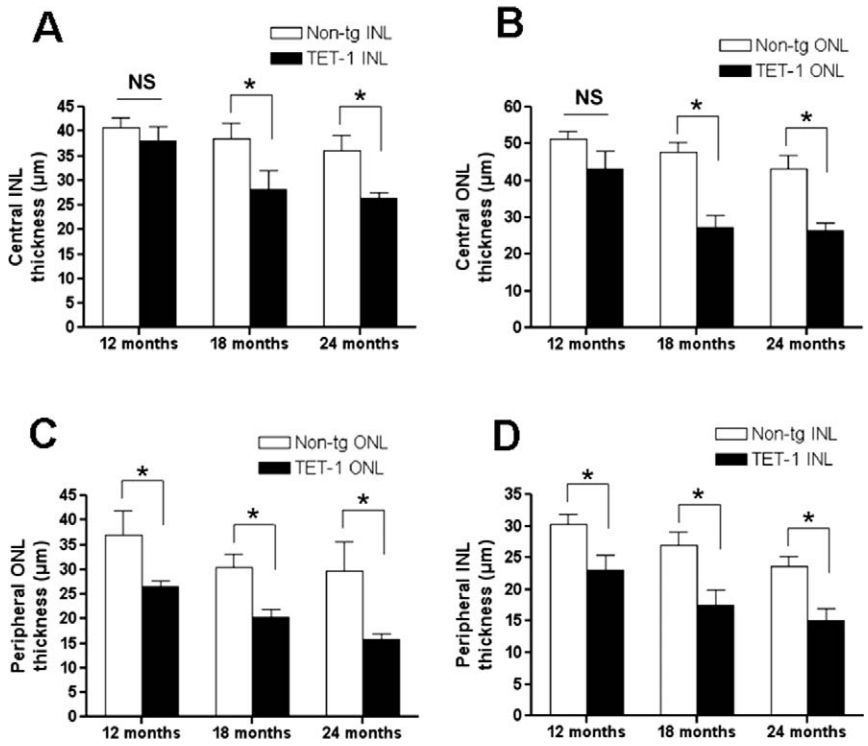

Figure 2. Thinning of retinal layers in TET-1 mice. (**A**) Analysis of INL thickness in the central retina. (**B**) Analysis of ONL thickness in the central retina. (**C**) Analysis of INL thickness in the peripheral retina. (**D**) Analysis of ONL thickness in the peripheral retina ($n = 7$, $^*P < 0.001$). NS, no significance.

Statistical Analysis

All data analysis was performed in a blinded manner. The values were present as mean ± SD. Student's *t*-test or one-way ANOVA followed by Bonferroni's post-test was used for analysis of the results, including the IOP measurement, cell counting, retinal layer thickness analysis, and glial fibrillary acidic protein (GFAP) staining intensity. Statistically significant difference was set at $P < 0.05$.

Results

Loss of RGCs and Thinning of Retinal Layers in TET-1 Mice

Our previous study has reported the upregulated mRNA and peptide expression of ET-1 in TET-1 mice.[29] Here, in H&E-stained retinal sections, 24-month-old TET-1 mice showed a decrease of cell density in the ganglion cell layer (GCL) in both the central and peripheral retina (Figs. 1B, 1D) when compared with the age-matched Non-tg controls (Figs. 1A, 1C). Quantitative analysis showed a progressive loss of neurons in the GCL in the early age of TET-1 mice when compared with the age-matched Non-tg ($n = 7$, $P < 0.001$) (Figs. 1G, 1H). At as early as 12 months of age, a significant neuronal loss in the GCL was first shown in the peripheral retina, whereas the cell density in the central GCL showed no significant decrease. At the age of 18 months, the cell density of GCL became smaller not only in the peripheral but also in the central retina. At 24 months, an obvious neuronal loss was shown in the TET-1 retina (32.1% in the central area and 35.7% in the peripheral area; $n = 7$, $P < 0.001$). These data suggested that in the TET-1 mice, the tendency of neuronal degeneration in the GCL started first from the peripheral retina and then spread to the central retina.

β-Tubulin III can be used as a marker to label RGCs.[21,22] Here we used it to distinguish RGCs from displaced amacrine cells in the GCL on retinal flat-mounts. Our results showed that there was a remarkable RGC loss at around 33.4 ± 5.7% in the 24-month-old TET-1 mice (2547 ± 218 cells/mm^2) compared with the Non-tg controls (3826 ± 152 cells/mm^2) ($n = 7$; $P < 0.001$) (Figs. 1E, 1F, 1I), a ratio similar to that seen in retinal sections.

To check if there is degeneration of other retinal neurons in the TET-1 mice, retinal layer thickness analysis was used. When compared with the age-matched Non-tg controls at each time point (12 months, 18 months, and 24 months), TET-1 mice showed a progressive thinning of the INL and ONL (Fig. 2). As early as the age of 12 months, a significant decrease of retinal thickness was detected in the peripheral INL and ONL (Figs. 2C, 2D); at the age of 18 months, a significant decrease of the INL and ONL was observed in both the peripheral and central retina (Figs. 2A, 2B); at the age of 24 months, the decrease of thickness became more obvious. These findings suggested that TET-1 mice showed a severe neuronal loss not only in the GCL but also in the INL and ONL. Thus, the aged TET-1 mice showed degeneration in many retinal layers.

Degeneration of Optic Nerve in the TET-1 Mice

Associating with the progressive loss of RGCs, 24-month-old TET-1 mice showed the attenuation of the retinal nerve fiber layer (NFL) (Fig. 3B) compared with the same aged Non-tg controls (Fig. 3A). Quantitative analysis showed the significant NFL thinning in the TET-1 mice (41.6%; $n = 7$, $P < 0.05$) at the central retina (200 μm from the optic nerve head) when compared with the Non-tg mice (Fig. 3C). The transverse section of the myelinated optic nerve showed the morphologic changes in the 24-month-old TET-1 mice, exhibiting the dense staining of the degenerating axons and many vacant holes

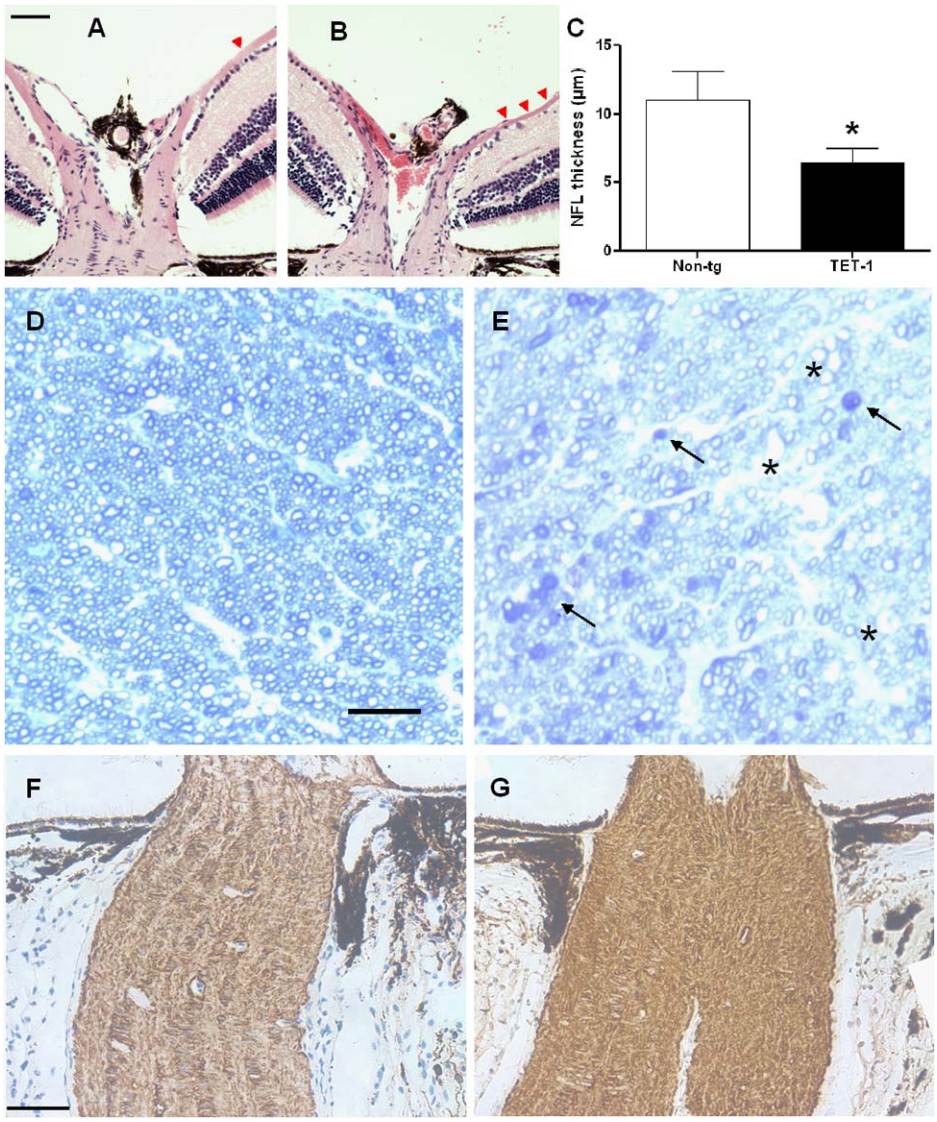

Figure 3. Optic nerve degeneration in 24-month TET-1 mice. (**A**, **B**) Representative photos of H&E-stained sections in Non-tg (**A**) and TET-1 mice (**B**). Sections illustrating the thinning of retinal nerve fiber layer (*arrowheads*) in the TET-1 mice compared with the Non-tg mice. (**C**) Quantitative analysis to show the significant difference in the thickness of the nerve fiber layer (NFL) in 24-month Non-tg mice and TET-1 mice ($n = 7$, $^*P < 0.001$). (**D**, **E**) Toluidin blue–stained cross-sections of axons in the mylinated optic nerve from the 24-month Non-tg (**D**) and TET-1 mice (**E**). Note that the dense staining shows the degenerating axon (*arrows*) and the holes (*asterisks*) show the position of the lost axons in (**E**). (**F**, **G**) GFAP-stained cross-sections of the optic nerve of Non-tg mice (**F**) and TET-1 mice (**G**). Scale bars: (**A**, **B**, **F**, **G**) 50 μm; (**D**, **E**) 20 μm.

replacing the lost axons (Fig. 3E). The increased expression of GFAP and the disarranged structure of astrocytes suggest the presence of astrocytosis in the TET-1 optic nerve (Fig. 3G) compared with the Non-tg mice (Fig. 3F). This is the corresponding reactivation of glial cells associating with the axonal degeneration of RGCs.

Normal IOP in the TET-1 Mice

To determine whether the IOP was affected in the TET-1 mice, IOP was measured at around 8 to 10 PM, near the peak of IOP in mouse eyes as reported previously.[28] No significant differences in the IOP level were detected between TET-1 mice and Non-tg mice in various ages, including the young (1–2 months), adult (10–16 months), and aged group (21–24 months). Different categories of sex (male and female) also displayed no significant changes in the IOP ($n = 10$–12 per sex per age; $P = 0.791$ by one-way ANOVA) (Fig. 4).

Increase of IgG-Leaked Blood Vessels in the TET-1 Mice

To detect whether increased endothelial ET-1 in the TET-1 mice has the effect on damaging the permeability of the microvessels, IgG staining was examined in the retinal sections. IgG leakage can be used to detect the damage of the blood-retinal-barrier (BRB), which has been used in previous studies.[24,30] Our study showed that a greater number of leaky blood vessels with immunopositive IgG signals located outside the endothelial vessel lining was observed in the 24-month-old TET-1 retina (Fig. 5B), when compared with the Non-tg control (Fig. 5A). Quantitative analysis showed there were significant differences both in the GCL and INL ($n = 7$, $P < 0.001$) (Fig. 5C). Western

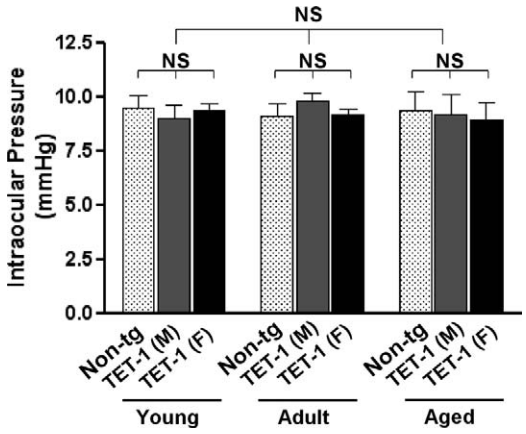

Figure 4. Normal IOP in TET-1 mice. There are no significant differences in the IOP between TET-1 mice and Non-tg mice in the young (1–2 months), adult (10–16 months), and aged group (21–24 months). Different categories of sex (male versus female) also exhibited no significant change of IOP ($n = 10$–12 per sex with per age; $P > 0.05$). NS, no significance; TET-1 (M), male TET-1 mice; TET-1 (F), female TET-1 mice.

blotting data showed there was a significantly decreased level of the occludin protein in the 24-month-old TET-1 retina compared with the Non-tg control ($n = 6$, $P < 0.001$) (Fig. 5D).

Remodeling of Retinal Microvasculature in TET-1 Mice

Using Isolectin B4, the main retinal arteries and veins were identified morphologically.[26] Here, we detected whether overexpression of endothelial ET-1 affects the retinal blood vasculature. The capillary networks were sparse in 24-month-old TET-1 mice (Fig. 6D), whereas it was abundant in Non-tg mice (Fig. 6A). The high-magnification micrographs showed more details of the sparse capillary network around the optic nerve head in TET-1 mice (Fig. 6E) compared with Non-tg mice (Fig. 6B). The sparse capillary networks were detected in the entire retina of TET-1 mice (Fig. 6F) compared with Non-tg mice (Fig. 6C). Further quantification (Figs. 6G vs. 6H) showed a significant decrease of capillary density in TET-1 retinas compared with Non-tg retinas (Fig. 6I). The branch points of retinal arteries were also significantly decreased in the superficial retina of TET-1 mice compared with Non-tg mice (Fig. 6J). The vascular loops were observed in TET-1 retinas (Fig. 6H), whereas no obvious looping formation was observed in vessels of Non-tg retina (Fig. 6G).

Reactivation of Astrocytes around Blood Vessels in the TET-1 Mice

Under normal conditions, GFAP is mostly expressed in the astrocytes of the GCL. Under stress, the expression of GFAP will be increased not only in astrocytes but also in the processes of the Müller cells seen clearly in retinal sections.[15,19,24,30] Thus, the increased expression of GFAP has been considered as an indication of retinal gliosis. Here, we showed that this change was also present in the TET-1 retina. In the 24-month-old TET-1 mice (Figs. 7B, 7D), the expression of GFAP was increased in the retinal sections when compared with the Non-tg mice (Figs. 7A, 7C). Semiquantitative analysis of GFAP immunointensity confirmed this tendency (Fig. 7E). Moreover, the 24-month-old TET-1 mice also showed the specific morphologic change in astrocytes on retinal flat-mounts, with complicated processes and enlargement of the

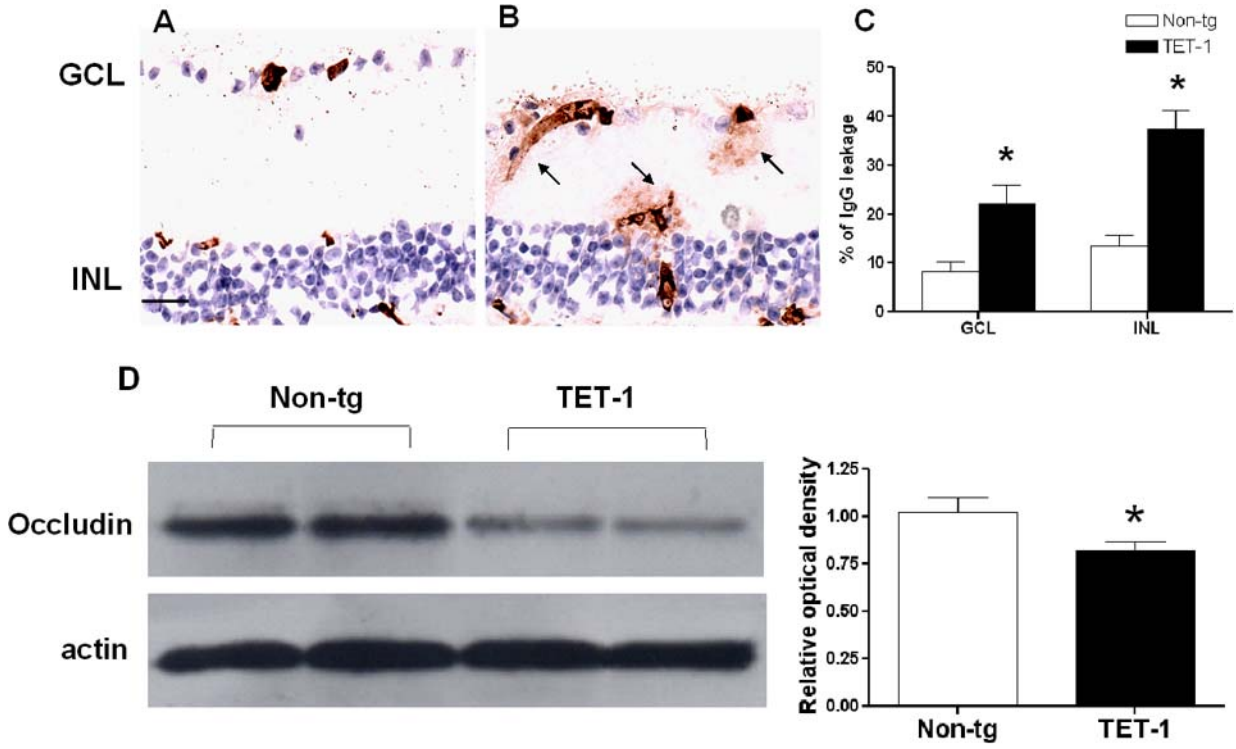

Figure 5. IgG leakage and decrease in occludin level in 24-month-old TET-1 retina. The *arrows* show the increased IgG leakage in the TET-1 mice (**B**) compared with the Non-tg mice (**A**). In both GCL and INL, there are more IgG-leaked blood vessels (*arrows*) found in TET-1 mice. (**C**) Quantitative analysis of IgG leakage in TET-1 mice and Non-tg mice ($n = 7$, $^*P < 0.001$) (**D**) Western blotting data of occludin level ($n = 6$, $^*P < 0.001$). Scale bar: 20 μm.

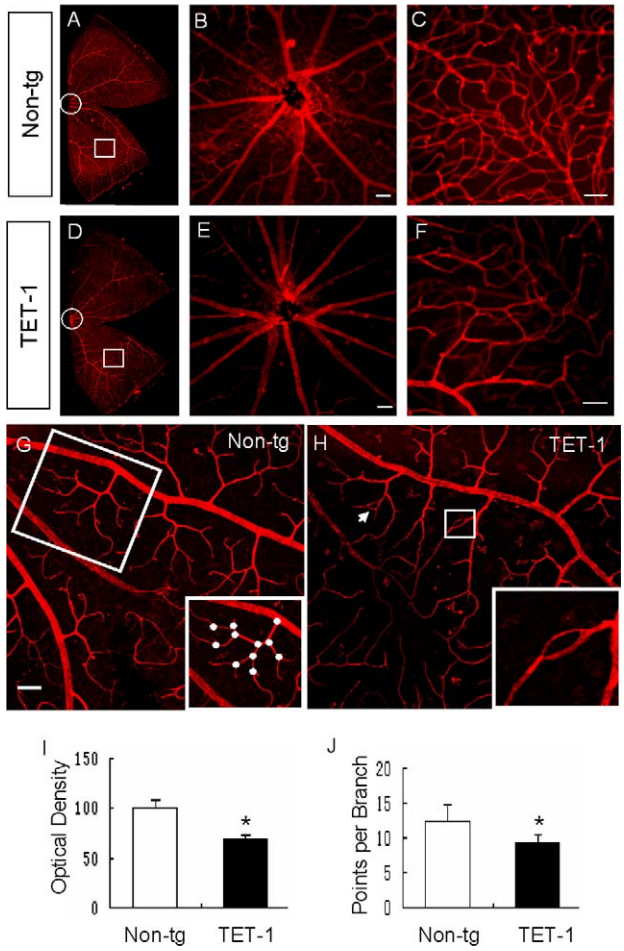

Figure 6. Morphologic changes of vasculature in 24-month-old TET-1 retina. (**A**–**F**) The representative profile of the retinal vasculature in Non-tg (**A**) and TET-1 group (**D**). The *circles* refer to the capillary network around the optic nerve head, enlarged in (**B**, **E**), and the *boxes* refer to the capillary network in the midperipheral retina, enlarged in (**C**, **F**). (**G**, **H**) Representative fluorescence photos show the morphologic analysis of retinal vasculature in the TET-1 group (**H**) compared with the Non-tg group (**G**). In (**G**), the *white dots* in the *box* show the graphic branch point analysis. In (**H**), the *arrow* shows the formation of a vascular loop. The enlarged photo in the *box* shows another vascular loop, which was not observed in the Non-tg retinas. (**I**, **J**) Quantitative analysis of the retinal vasculature. In the bar chart (**I**), the value of the optical intensity illustrates the decrease of microvessel density in the TET-1 mice. The bar chart (**J**) shows that the branch points produced from the main retinal arteries were decreased in the TET-1 mice when compared with the Non-tg mice ($n = 5$, $^*P < 0.001$). Scale bar: 50 μm.

end-feet located around the blood vessels (Figs. 7I–K); however, this phenomenon was not obvious in the age-matched Non-tg retina (Figs. 7F–H). The enlarged photographs showed this phenomenon more clearly (Figs. 7L vs. 7M).

Discussion

Here, we demonstrated that with overexpressing ET-1 in the vascular endothelial cells, TET-1 mice showed a progressive neurodegeneration in the retina without elevation of IOP. Loss of RGCs and neurons in the INL and ONL associated with optic neuropathy during aging was observed. These data showed, for the first time, that the long-term overexpression of endothelial ET-1 could damage the retinal tissue and optic nerve.

Relationship of TET-1 Mice with NTG and Other Vascular-Related Retinal Diseases

Elevated levels of ET-1 in plasma have been reported in the TET-1 mice in our previous study,[31] which is similar to clinical findings reported in some population of NTG.[6–8] Many lines of evidence indicated that ET-1 was involved in the pathogenesis of neurodegeneration of NTG both in clinic and in nonhuman animal studies.[5–8] Here, we investigated the morphologic changes of retina induced by overexpression of endothelial ET-1. TET-1 mice showed progressive loss of RGCs and degeneration of their axons, which are two key phenotypes of NTG.[32] However, some phenotypes were also observed that were different from clinical NTG findings, such as no flat-bottomed cupping and the presence of neuronal loss in the INL and ONL.

First, in animal studies, plate-bottomed glaucomatous cupping was observed in the high-IOP–induced glaucoma model, such as nonhuman primates[33,34] and DBA/2J mice,[35] which is consistent with the finding of clinical glaucoma. However, this classical optic nerve excavation is absent in recently reported NTG-related mouse model, such as glutamate/aspartate transporter deficient (GLASTER–/–) mice,[36] OPTN gene mutated mice,[37] and WD repeat-containing protein 36 (WDR36) transgenic mice.[38] In our study, the thinning of NFL found in the aged TET-1 mice was in agreement with the findings in those gene-mutated normal-IOP mice.

The development of optic nerve excavation, the specific glaucomatous cupping shape with a flat bottom in patients with NTG may be related to elevation of IOP. This is supported in reports that lowering IOP treatment is effective in patients with NTG.[39] Moreover, thinner values of central corneal thickness (CCT) were found in patients with NTG than the mean corneal thickness in that population,[40] resulting in underestimation of the IOP reading and masking the sign of elevated IOP presented in patients with NTG. Together, it is believed that glaucomatous excavation is closely related to elevation of IOP, which made the cupping shape found in NTG-related animals different from that in high-IOP–induced animals.

Second, the presence of neuronal loss in the INL and ONL in the TET-1 mice may be related to the action sites of ET-1. Previous reports using ET-1 retroglobal delivery showed only the loss of RGCs in retina.[14,41] However, intravitreal injections of ET-1 induced degeneration not only in RGCs but also in neurons of the INL.[12,16] In our case, endothelial ET-1 could exert bioeffects along with the distribution of retinal blood vessels and aggravate the retinal degeneration by the leakage of BRB. Thus, the long-term effects and broad action sites of ET-1 in the TET-1 mice could be exhibited not only on RGCs but also on other retinal neurons. This pattern of many layer retinal degeneration is in agreement with that of previously reported NTG-related mouse model of OPTN mutated mice and WRD36 mutated mice.[37,38] Our data showing BRB damage in the TET-1 mice suggested that overexpression of endothelial ET-1 may be a cause of BRB damage found in the patients with NTG and POAG.[42,43] In addition, dysfunction of photoreceptors was reported recently in some advanced glaucoma patients and in glaucoma animal model of ocular hypertension, indicating loss of RGCs may not be the only neural degeneration in the pathogenesis of glaucoma.[44,45]

Taken together, it may be indicated that NTG-like animals not only contain similar features as clinical NTG but also other different phenotypes due to their specific pathogenesis of gene mutation.

Other vascular-related retinal degenerative diseases, such as age-related macular degeneration (ARMD), were also considered in our study. We carefully checked the histologic sections

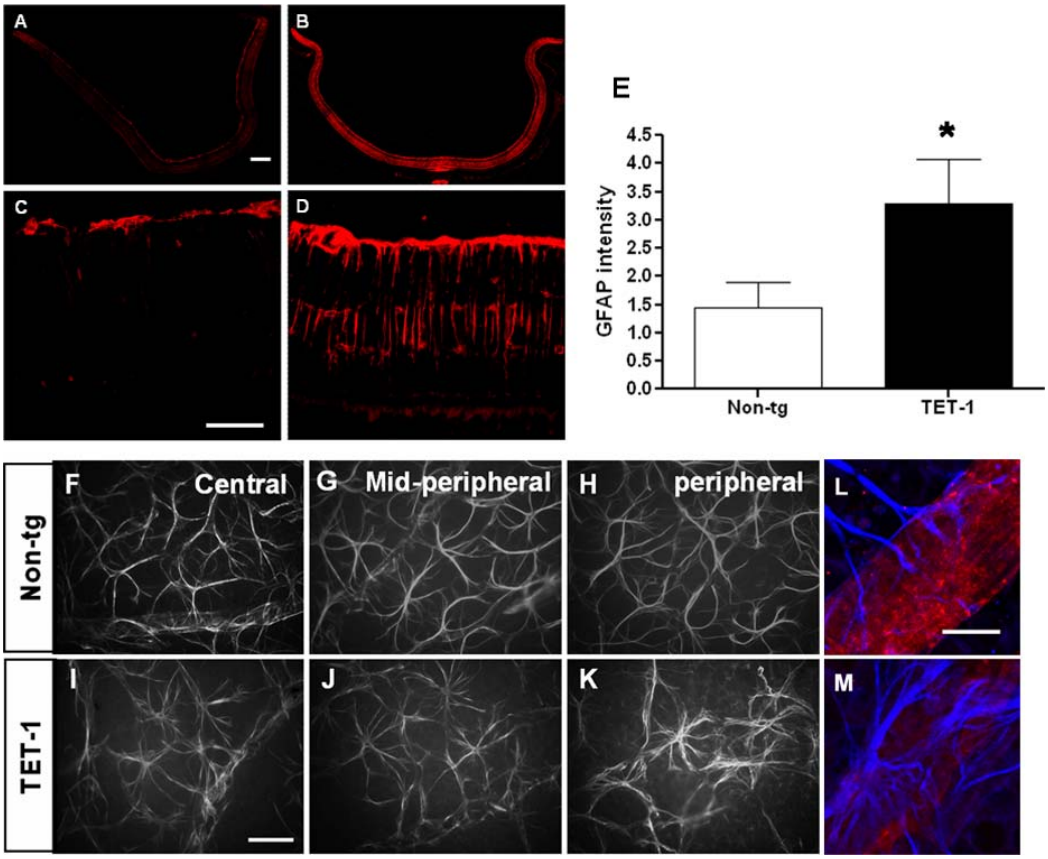

Figure 7. Retinal gliosis in the 24-month-old TET-1 mice. (**A–D**) GFAP-stained retinal cross-section of the Non-tg mice (**A**) and its enlarged photo (**C**); GFAP-stained retinal cross-section of the TET-1mice (**B**) and its enlarged photo (**D**). (**E**) The semiquantitative analysis of GFAP staining in 24-month animals ($n = 7$, $^*P < 0.001$). (**F–K**) The morphologic change of retinal astrocytes around the blood vessels in different areas of flat-mounted retinas in the Non-tg mice (**F–H**) and TET-1 mice (**I–K**). (**L**, **M**) The detailed end-feet change in the TET-1 retina (**M**) compared with the Non-tg (**L**) from midperipheral retina by confocal microscopy with isolectin-B4–labeled blood vessels (*red*) and GFAP-labeled astrocytes (*blue*). Scale bars: (**A–D**, **F–K**) 50 μm; (**L**, **M**) 10 μm.

of TET-1 mice and observed that except for a mild increase of autofluorescence in retinal pigment epithelium cells (RPEs), there was no sign of the classic ARMD-related retinopathy in aged TET-1 mice, such as drusen deposition, RPE degeneration, thickening of Bruch's membrane, and characteristic choriocapillaris (CNV),[46] suggesting exclusion of ARMD-related retinopathy (data not shown). Breakdown of BRB is a key event in ischemic retinopathy,[30] such as diabetic retinopathy (DR). However, we also checked the structure of retinal vasculature using isolectin B4 staining and excluded neovascularization[26] in TET-1 retina (data not shown). Our previous study reported the mild elevation of systolic blood pressure exhibited in TET-1 mice.[31] Thus, in this study, we also performed fundus examination in TET-1 mice during IOP measurement at various ages. However, we did not find obvious signs of hypertensive retinopathy (HR), such as tortuous arteries, artery–vein nipping, hemorrhages, or any formed retinal extrusions. Isolectin B4 staining showed negative HR-related vascular changes in TET-1 retina. Taken together, it is suggested that the presence of IgG leakage and BRB breakdown in normal aging TET-1 mice may not be severe enough to produce formed exudates and neovascularization, as seen in diabetic or other retinopathy. However, the leaky blood vessels in TET-1 retina may indicate exuding of proteins, inflammatory factors, and other deleterious molecules from BRB into retinal tissue, which is detrimental to the survival of retinal neurons. In addition, we cannot exclude that hypertension may play a role in the injury of retinal blood vessels and the neurons in TET-1 mice for its aggravating effects reported in cerebral ischemia.[18,47]

Possible Role of Endothelial ET-1 in the Neurodegeneration of Retina

From the preceding discussions, it could be summarized that in the TET-1 mice, endothelial ET-1 induces or contributes to retinal neurodegeneration through four pathways: hypoxia/ischemia damage, BRB damage, retinal gliosis, and inducing RGC death directly.

As a potent vasoconstrictor, ET-1 induced the damage in the optic nerve and retina via the ischemia/reperfusion (I/R) injury.[11,12,16] Our previous studies also showed ET-1 could aggravate brain and retina damage in a middle artery occlusion (MCAO)–induced I/R injury by using the TET-1 mice.[17,18,29,48,49] This study is the first to show endothelial ET-1–induced microvascular remodeling, such as vascular loop formation and decrease of capillary network in the retina of TET-1 mice. As a hallmark of intussusceptive angiogenesis (IA),[50] loop formation was reported in adult mouse retina induced by chronic whole-body hypoxia,[26] which suggested the similar mechanism of chronic hypoxia occurring in TET-1 retina. This is different from the classic mode of sprouting angiogenesis (SA), found in ARMD and DR. The IA, as indicated by the loop formation found in TET-1 mice, might belong to a

hypoxia-adaptation mechanism,[50] which could be able to oppose the diminishing capillary network as reported in our finding. Further work is needed to investigate molecular signaling pathways to evaluate the adaptation/deadaptation mechanism of hypoxia involved in TET-1 retina. The result in this work provided the morphologic evidence that overexpression of endothelial ET-1 leads to altered microvasculature and contributes to retinal degeneration.

ET-1 has the effect of destroying the integrity of BRB by reducing the function of the endothelial tight-junction complex.[18,48] BRB damage enables the access of circulating molecules in the blood, such as ET-1 and glutamate, which can trigger inflammation, oxidative stress, perivascular edema, and axonal demyelination.[51]

Astrocytes have been suggested as a target of ET-1. ET-1–induced activation of astrocytes in the optic nerve head was considered as a deleterious effect.[29,41,52,53] The mice with overexpression of ET-1 in the astrocytes (GET-1 mice) showed that astrocytic ET-1 has deleterious effects on water homeostasis, cerebral edema, and BBB integrity, which worsened the ischemic brain injury.[48] A previous study reported that the complicated processes of retinal astrocytes was observed as an aging sign of rat retina.[54] However, the enlargement of the end-feet of retinal astrocytes around blood vessels was much more often observed in the aged TET-1 mice than in the aged Non-tg mice, suggesting an effect of overexpressed ET-1 on astrocytes in our study. One of the possibilities of this phenomenon is end-feet edema, which may suggest the functional deficiency of BRB in the TET-1 mice.

ET-1 can affect RGCs directly by three lines of evidences. First, there are ET-1 receptors, ET_A and ET_B expressed on RGCs[55]; second, there is evidence shown in the culture system that ET-1 could mediate the apoptosis of RGC-5 cells directly[56]; and third, ET-1 could induce apoptosis of RGCs in the in vivo animal model of ET-1–induced ischemia in the optic nerve head.[14]

In summary, the phenotype of the TET-1 mice involves the major morphologic changes including the loss of RGCs, thinning of INL, ONL, NFL, and the degeneration of optic axons, together with the blood vessel changes and retinal gliosis. Taken together, our transgenic mice with endothelial cell–specific overexpression of ET-1 would serve as a useful model for understanding the effect of long-term exposure of endothelial ET-1 in microvascular remodeling and retinal degeneration.

References

1. McKinnon SJ. Glaucoma: ocular Alzheimer's disease. *Front Biosci*. 2003;8:s1140–s1156.
2. Klein BE, Klein R, Sponsel WE, et al. Prevalence of glaucoma. The Beaver Dam Eye Study. *Ophthalmology*. 1992;99:1499–1504.
3. Iwase A, Suzuki Y, Araie M, et al. The prevalence of primary open-angle glaucoma in Japanese: the Tajimi Study. *Ophthalmology*. 2004;111:1641–1648.
4. Cursiefen C, Wisse M, Cursiefen S, Jünemann A, Martus P, Korth M. Migraine and tension headache in high-pressure and normal-pressure glaucoma. *Am J Ophthalmol*. 2000;129:102–104.
5. Yorio T, Krishnamoorthy R, Prasanna G. Endothelin: is it a contributor to glaucoma pathophysiology? *J Glaucoma*. 2002;11:259–270.
6. Cellini M, Possati G, Profazio V, Sbrocca M, Caramazza N, Caramazza R. Color Doppler imaging and plasma levels of endothelin-1 in low-tension glaucoma. *Acta Ophthalmol Scand*. 1997;75:11–13.
7. Sugiyama T, Moriya S, Oku H, Azuma I. Association of endothelin-1 with normal tension glaucoma: clinical and fundamental studies*. *Surv Ophthalmol*. 1995;39:S49–S56.
8. Emre M, Orgül S, Haufschild T, Shaw SG, Flammer J. Increased plasma endothelin-1 levels in patients with progressive open angle glaucoma. *Br J Ophthalmol*. 2005;89:60–63.
9. Grieshaber MC, Mozaffarieh M, Flammer J. What is the link between vascular dysregulation and glaucoma? *Surv Ophthalmol*. 2007;52:S144–S154.
10. Galassi F, Giambene B, Varriale R. Systemic vascular dysregulation and retrobulbar hemodynamics in normal-tension glaucoma. *Invest Ophthalmol Vis Sci*. 2011;52:4467–4471.
11. Orgül S, Cioffi GA, Bacon DR, Van Buskirk EM. An endothelin-1-induced model of chronic optic nerve ischemia in rhesus monkeys. *J Glaucoma*. 1996;5:135–138.
12. Nagano H, Wei PZ, Wen CQ, et al. Effects of kallidinogenase on ischemic changes induced by repeated intravitreal injections of endothelin-1 in rabbit retina. *Curr Eye Res*. 2007;32:113–122.
13. Taniguchi T, Shimazawa M, Sasaoka M, Shimazaki A, Hara H. Endothelin-1 impairs retrograde axonal transport and leads to axonal injury in rat optic nerve. *Curr Neurovasc Res*. 2006;3:81–88.
14. Chauhan BC, LeVatte TL, Jollimore CA, et al. Model of endothelin-1-induced chronic optic neuropathy in rat. *Invest Ophthalmol Vis Sci*. 2004;45:144–152.
15. Lau J, Dang M, Hockmann K, Ball AK. Effects of acute delivery of endothelin-1 on retinal ganglion cell loss in the rat. *Exp Eye Res*. 2006;82:132–145.
16. Sasaoka M, Taniguchi T, Shimazawa M, Ishida N, Shimazaki A, Hara H. Intravitreal injection of endothelin-1 caused optic nerve damage following to ocular hypoperfusion in rabbits. *Exp Eye Res*. 2006;83:629–637.
17. Leung JWC, Ho MCY, Lo ACY, Chung SSM, Chung SK. Endothelial cell-specific over-expression of endothelin-1 leads to more severe cerebral damage following transient middle cerebral artery occlusion. *J Cardiovasc Pharmacol*. 2004;44(suppl 1):S293–S300.
18. Leung JWC, Chung SSM, Chung SK. Endothelial endothelin-1 over-expression using receptor tyrosine kinase tie-1 promoter leads to more severe vascular permeability and blood brain barrier breakdown after transient middle cerebral artery occlusion. *Brain Res*. 2009;1266:121–129.
19. Li SY, Fu ZJ, Ma H, et al. Effect of lutein on retinal neurons and oxidative stress in a model of acute retinal ischemia/reperfusion. *Invest Ophthalmol Vis Sci*. 2009;50:836–843.
20. Cheung AKH, Lo ACY, So KF, Chung SSM, Chung SK. Gene deletion and pharmacological inhibition of aldose reductase protect against retinal ischemic injury. *Exp Eye Res*. 2007;85:608–616.
21. Cui Q, Hodgetts S, Hu Y, Luo JM, Harvey A. Strain-specific differences in the effects of cyclosporin A and FK506 on the survival and regeneration of axotomized retinal ganglion cells in adult rats. *Neuroscience*. 2007;146:986–999.
22. Chen H, Wei X, Cho KS, et al. Optic neuropathy due to microbead-induced elevated intraocular pressure in the mouse. *Invest Ophthalmol Vis Sci*. 2011;52:36–44.
23. Fu QL, Hu B, Wu W, Pepinsky RB, Mi S, So KF. Blocking LINGO-1 function promotes retinal ganglion cell survival following ocular hypertension and optic nerve transection. *Invest Ophthalmol Vis Sci*. 2008;49:975–985.
24. Li S-Y, Yang D, Yeung C-M, et al. *Lycium barbarum* polysaccharides reduce neuronal damage, blood-retinal barrier disruption and oxidative stress in retinal ischemia/reperfusion injury. *PloS ONE*. 2011;6:e16380.
25. Mori A, Saigo O, Hanada M, Nakahara T, Ishii K. Hyperglycemia accelerates impairment of vasodilator responses to acetylcho-

line of retinal blood vessels in rats. *J Pharmacol Sci*. 2009;110: 160–168.

26. Taylor AC, Seltz LM, Yates PA, Peirce SM. Chronic whole-body hypoxia induces intussusceptive angiogenesis and microvascular remodeling in the mouse retina. *Microvasc Res*. 2010;79:93–101.
27. Chacón M, Barria M, Lorca R, Huidobro-Toro J, Inestrosa N. A human prion protein peptide (PrP(59–91)) protects against copper neurotoxicity. *Mol Psychiatry*. 2003;8:853–862.
28. Aihara M, Lindsey JD, Weinreb RN. Twenty-four-hour pattern of mouse intraocular pressure. *Exp Eye Res*. 2003;77:681–686.
29. Cheung SS, Leung JW, Lam AK, et al. Selective over-expression of endothelin-1 in endothelial cells exacerbates inner retinal edema and neuronal death in ischemic retina. *PLoS ONE*. 2011;6:e26184.
30. Cheung AKH, Fung MKL, Lo ACY, et al. Aldose reductase deficiency prevents diabetes-induced blood-retinal barrier breakdown, apoptosis, and glial reactivation in the retina of *db/db* mice. *Diabetes*. 2005;54:3119–3125.
31. Leung JW, Wong WT, Koon HW, et al. Transgenic mice over-expressing ET-1 in the endothelial cells develop systemic hypertension with altered vascular reactivity. *PLoS ONE*. 2011; 6:e26994.
32. Shields MB. Normal-tension glaucoma: is it different from primary open-angle glaucoma? *Curr Opin Ophthalmol*. 2008; 19:85–88.
33. Gaasterland D, Kupfer C. Experimental glaucoma in the rhesus monkey. *Invest Ophthalmol*. 1974;13:455–457.
34. Quigley HA. Glaucoma. *Lancet*. 2011;377:1367–1377.
35. John S, Smith RS, Savinova OV, et al. Essential iris atrophy, pigment dispersion, and glaucoma in DBA/2J mice. *Invest Ophthalmol Vis Sci*. 1998;39:951–962.
36. Harada T, Harada C, Nakamura K, et al. The potential role of glutamate transporters in the pathogenesis of normal tension glaucoma. *J Clin Invest*. 2007;117:1763–1770.
37. Chi ZL, Akahori M, Obazawa M, et al. Overexpression of optineurin E50K disrupts Rab8 interaction and leads to a progressive retinal degeneration in mice. *Hum Mol Genet*. 2010;19:2606–2615.
38. Chi ZL, Yasumoto F, Sergeev Y, et al. Mutant WDR36 directly affects axon growth of retinal ganglion cells leading to progressive retinal degeneration in mice. *Hum Mol Genet*. 2010;19:3806–3815.
39. Shah R, Wormald RP. Glaucoma. *Clin Evid (Online)*. 2011;Jun 9:2011.
40. Kniestedt C, Lin S, Choe J, et al. Correlation between intraocular pressure, central corneal thickness, stage of glaucoma, and demographic patient data: prospective analysis of biophysical parameters in tertiary glaucoma practice populations. *J Glaucoma*. 2006;15:91–97.
41. Wang X, LeVatte TL, Archibald ML, Chauhan BC. Increase in endothelin B receptor expression in optic nerve astrocytes in endothelin-1 induced chronic experimental optic neuropathy. *Exp Eye Res*. 2009;88:378–385.
42. Schwartz B. Circulatory defects of the optic disk and retina in ocular hypertension and high pressure open-angle glaucoma. *Surv Ophthalmol*. 1994;38(suppl):S23–S34.
43. Grieshaber MC, Flammer J. Does the blood-brain barrier play a role in glaucoma? *Surv Ophthalmol*. 2007;52:S115–S121.
44. Heiduschka P, Julien S, Schuettauf F, Schnichels S. Loss of retinal function in aged DBA/2J mice: new insights into retinal neurodegeneration. *Exp Eye Res*. 2010;91:779–783.
45. Kanis MJ, Lemij HG, Berendschot TTJM, van de Kraats J, van Norren D. Foveal cone photoreceptor involvement in primary open-angle glaucoma. *Graefes Arch Clin Exp Ophthalmol*. 2010;248:999–1006.
46. Zhao Z, Chen Y, Wang J, et al. Age-related retinopathy in NRF2-deficient mice. *PLoS ONE*. 2011;6:e19456.
47. Tang Y, Li X, Li Y, et al. Renovascular hypertension causes cerebral vascular remodeling. *Neural Regen Res*. 2011;6: 1977–1981.
48. Lo ACY, Chen AYS, Hung VKL, et al. Endothelin-1 overexpression leads to further water accumulation and brain edema after middle cerebral artery occlusion via aquaporin 4 expression in astrocytic end-feet. *J Cereb Blood Flow Metab*. 2005;25:998–1011.
49. Yeung PKK, Lo ACY, Leung JWC, Chung SSM, Chung SK. Targeted overexpression of endothelin-1 in astrocytes leads to more severe cytotoxic brain edema and higher mortality. *J Cereb Blood Flow Metabolism*. 2009;29:1891–1902.
50. Makanya AN, Hlushchuk R, Djonov VG. Intussusceptive angiogenesis and its role in vascular morphogenesis, patterning, and remodeling. *Angiogenesis*. 2009;12:113–123.
51. Farrall AJ, Wardlaw JM. Blood-brain barrier: ageing and microvascular disease-systematic review and meta-analysis. *Neurobiol Aging*. 2009;30:337–352.
52. Prasanna G, Krishnamoorthy R, Clark AF, Wordinger RJ, Yorio T. Human optic nerve head astrocytes as a target for endothelin-1. *Invest Ophthalmol Vis Sci*. 2002;43:2704–2713.
53. Murphy JA, Archibald ML, Chauhan BC. The role of endothelin-1 and its receptors in optic nerve head astrocyte proliferation. *Br J Ophthalmol*. 2010;94:1233–1238.
54. Mansour H, Chamberlain CG, Weible I, et al. Aging-related changes in astrocytes in the rat retina: imbalance between cell proliferation and cell death reduces astrocyte availability. *Aging Cell*. 2008;7:526–540.
55. Torbidoni V, Iribarne M, Ogawa L, Prasanna G, Suburo AM. Endothelin-1 and endothelin receptors in light-induced retinal degeneration. *Exp Eye Res*. 2005;81:265–275.
56. Krishnamoorthy RR, Rao VR, Dauphin R, Prasanna G, Johnson C, Yorio T. Role of the ETB receptor in retinal ganglion cell death in glaucoma. *Can J Physiol Pharmacol*. 2008;86:380–393.